Direct N-body modeling of the outer halo globular clusters Palomar 14 and Palomar 4:

the eccentric orbit approach

Akram Hasani Zonoozi

Institute for Advanced Studies in Basic Sciences (IASBS)

Zanjan, IRAN

In collaboration with

H. Haghi, A. Kuepper H. Baumgardt , P. Kroupa, M. Frank

Dynamical Evolution of a Globular Cluster is driven by various mechanisms:

- **Stellar evolution**: Mass loss (about 30% of the cluster mass) form the cluster via supernova explosion and causes the GC to expand.
- **2-body Relaxation**: Energy exchange between two stars
- **External tidal perturbations**: Lowers the escape velocity from the GC
  - **Disk/bulge shocks**: Rapid change in external potential heats GCs
  - **Eccentric cluster orbits**: Causes GCs to experience deep and shallow external potentials alternatively

Realistic globular cluster simulation

- Long term evolution of Star clusters using direct N-body computation: Vespersini & Heggie 1997 (4K particles), Baumgardt & Makino 2003 (100K particles)

- Within the last few years it has become possible to compute the dynamical evolution of realistic globular clusters over entire lifetime: Zonoozi et al 2011 (Pal 14), Zonoozi et al 2014 (Pal 4)

Realistic globular cluster simulation

The Challenge of Milky Way Globular Clusters for *N*-body

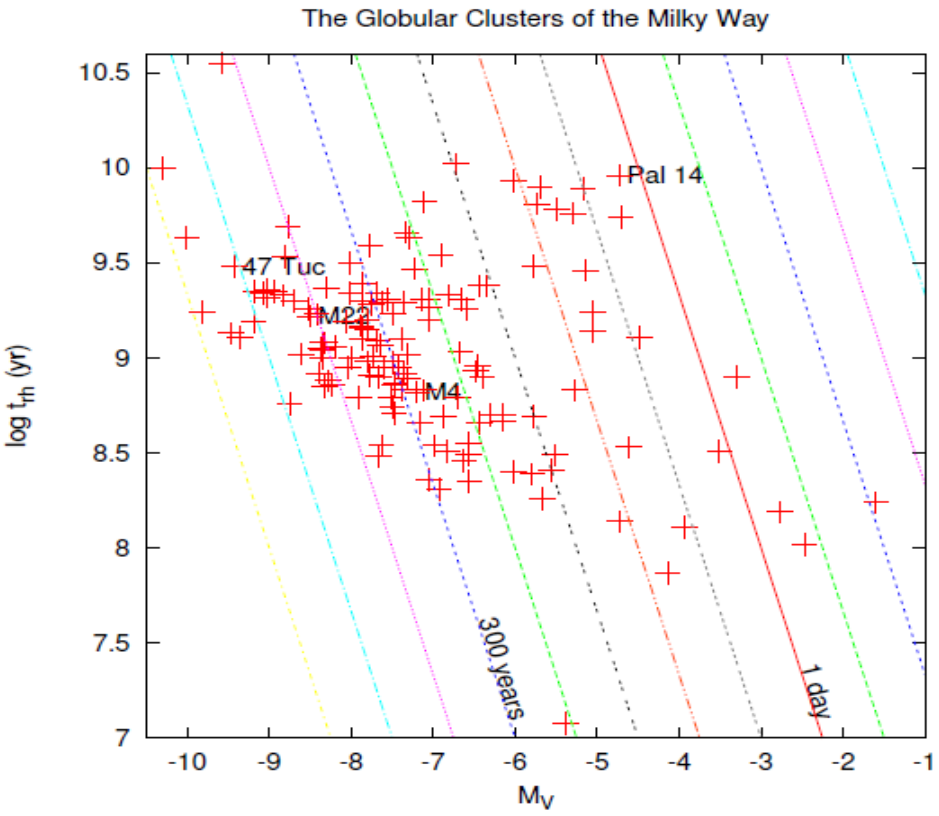

Taken from Heggie

Low mass together with large radius make possible to simulate these clusters on a star-by-star basis with **GPU-accelerated N-body6 code**.

Numerical Modeling:
Direct N-body simulation

I. Modeling of Palomar 14

Zonoozi et al 2011, MNRAS

II. Modeling of Palomar 4

Zonoozi et al 2014, MNRAS

Some interesting features of Palomar 4 and Palomar 14

Present day Mass Function slope

Pal 4: Frank et al. (2012)

$$0.55 \leq m/\mathrm{M}_{\odot} \leq 0.85$$

$$\alpha = 1.4 \pm 0.25$$

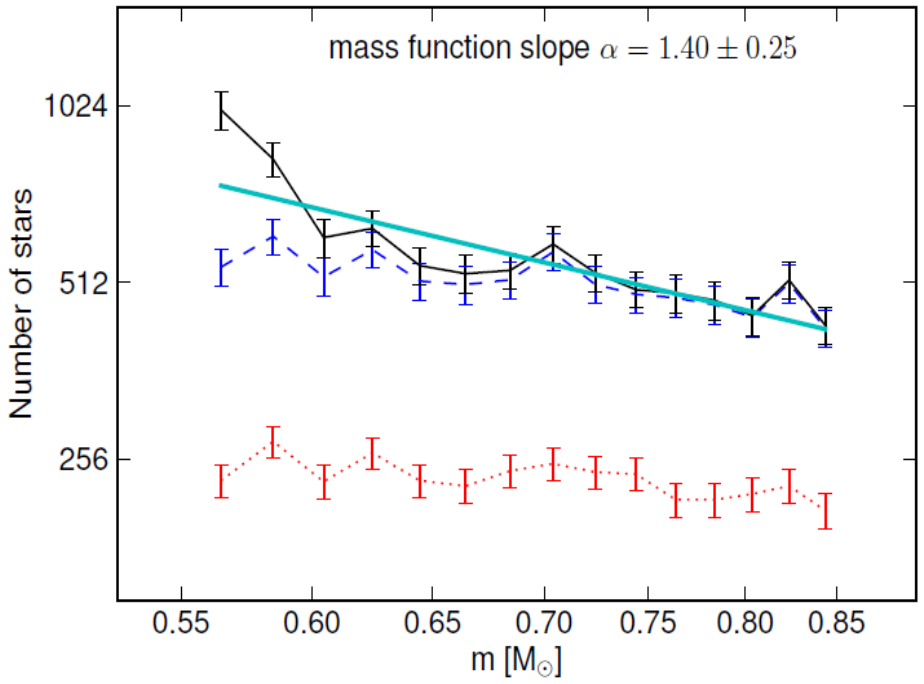

Pal 14: Jordi et al. (2009)

$$0.525\,M_{sun} < M < 0.79\,M_{sun}$$

$$\alpha = 1.27 \pm 0.44$$

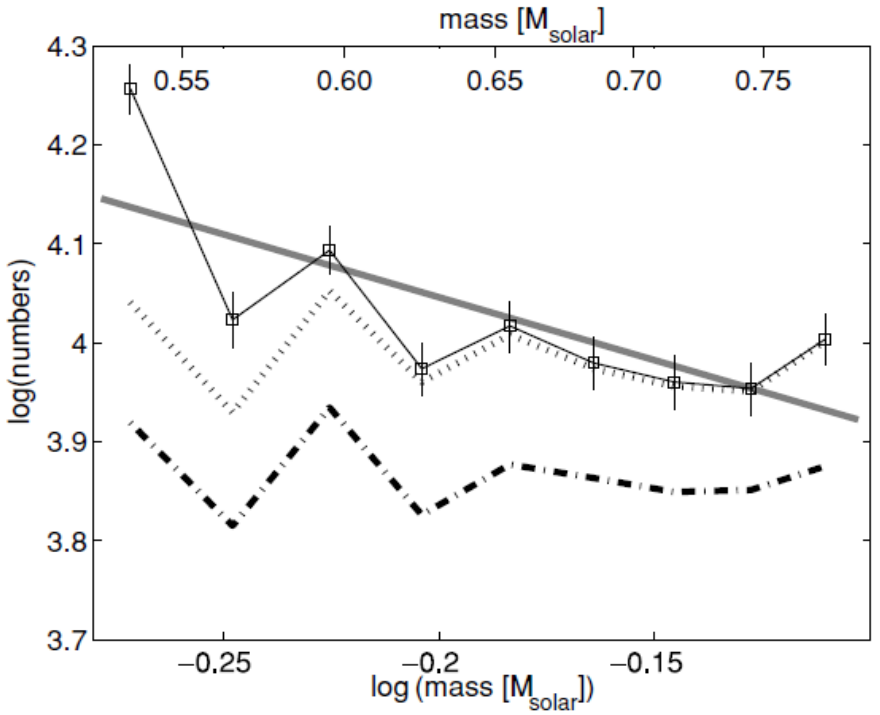

Flatter than Canonical Kroupa IMF $\alpha = 2.35$

Evolution of Mass Function

The mass function of stars in clusters evolves through stellar & dynamical evolution.

(Vesperini, Heggie 1997 , Baumgardt & Makino 2003)

Flattening of the mass function of GCs

Mass-function slope is a tracer of mass loss

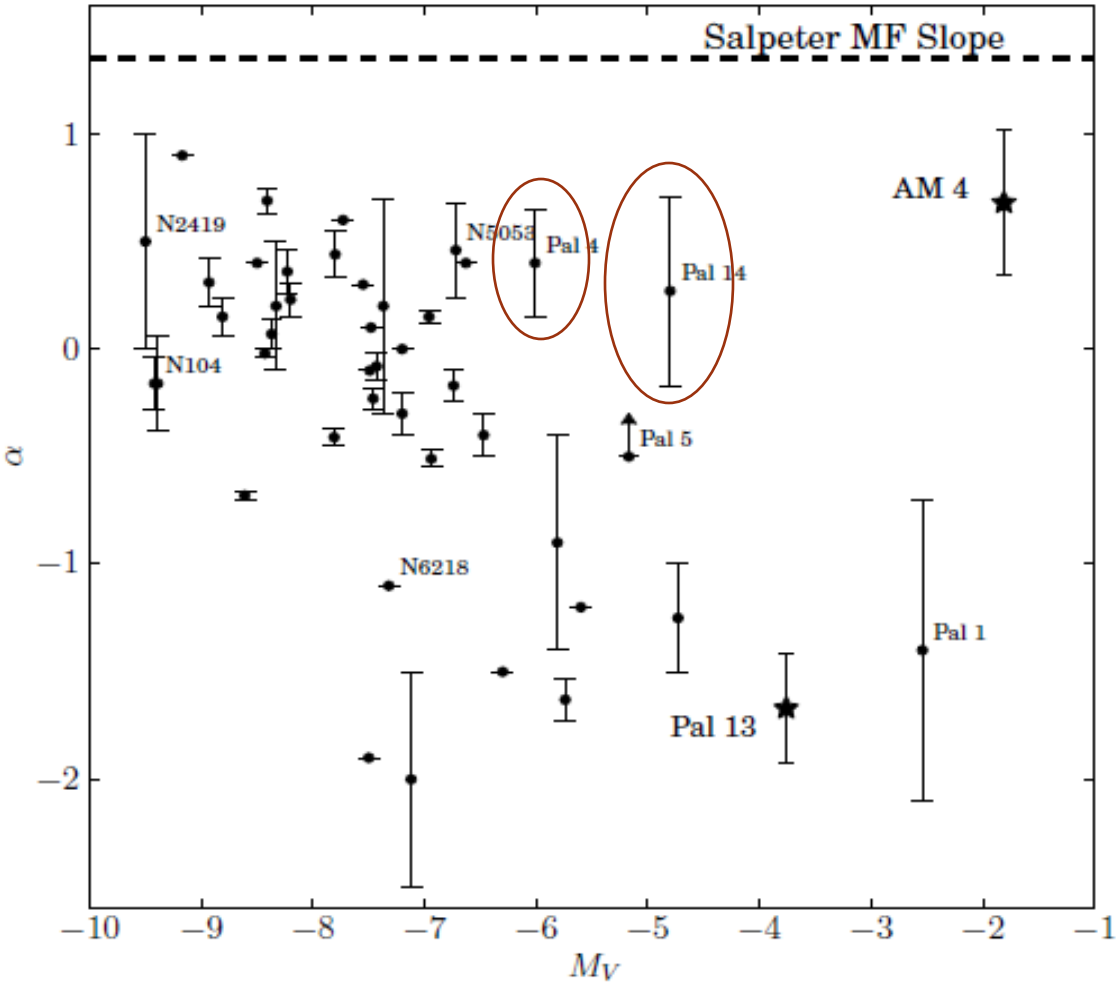

Hamren et al., 2013, ApJ

This is contrary to expectations since the driver of low-mass star depletion, two-body relaxation, should be least efficient in clusters with large Trh.

Highly mass segregated

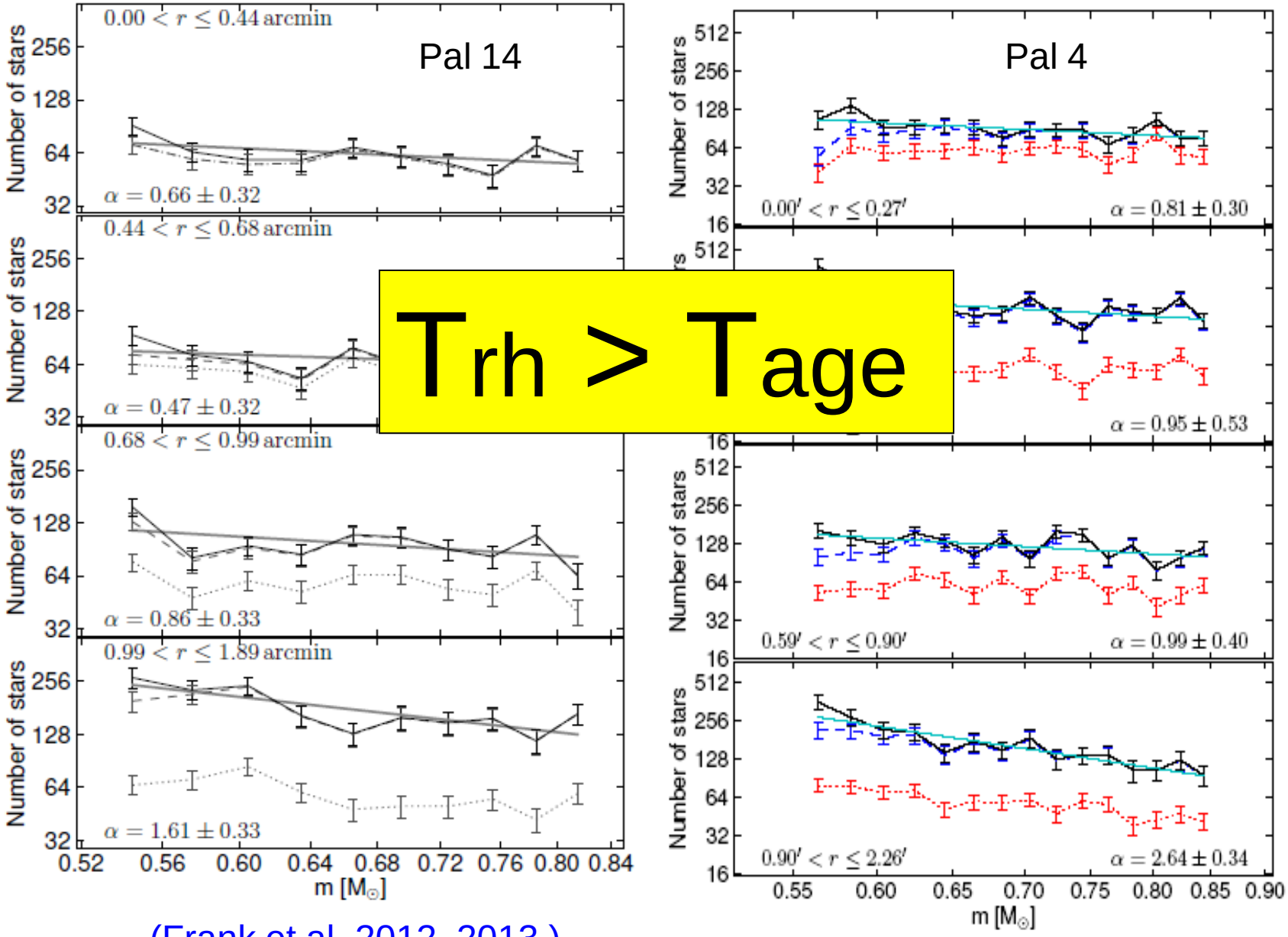

(Frank et al. 2012, 2013)

Direct N-body simulation

DESCRIPTION OF THE MODELS

We use the Aarseth's Nbody6 code on the GPU computers of the University of Bonn and the University of Queensland.

- Initial mass: [40-60]*1000 soalr mass
- Initial radius [8-15] pc
- N=100,000 stars, distributed with Plummer model
- Evolution time: T=12 Gyrs
- Metalicity: Z~0.001
- Stellar Evolution: SSE/BSE routines (Hurley et al. 2001)
- Tidal effect: galactic potential (Allen & Santillan 1991)
- **MCLUSTER** to set up initially segregated clusters (Keupper et al 2010)

Observational data

Pal 14 (Hilker 2006, Jordi et al 2009)

- Spectroscopic and photometric data
- Age: 11.5±0.5 Gyr
- Distance: 71± 1.3 kpc
- Half-light radius = 26 pc
- CDM: containing 3878 stars
- Number of bright stars: 2954±175
- Number of giants: 197±28
- Velocity dispersion: 0.87 ± 0.18 km/s

(radial velocity of 17 giant stars)

Pal 4 (Frank et al 2012)

- Spectroscopic and photometric data
- Age: 11±1 Gyr
- Distance:102± 2.4 kpc
- Half-light radius = 18.4 ± 2.0 pc
- Total mass = 29800 ± 800
- Velocity dispersion: 0.87 ± 0.18 km/s

(radial velocity of 23 giant stars)

Several scenarios for Initial conditions

Scenario1: Kroupa IMF – **Pal 14**

Model	R_{phm}[pc] (±0.8)	R_{phl}[pc] (±2.3)	N_{bs} (±260)	$M^{f}_{r<R_{hm}}$[$M_\odot$] (±320)	α (±0.15)	σ_{los}[km/sec] (±0.01)	N_g (±16)
M40R15	19.6	15.6	2374	1521	2.10	0.65	162
M40R25	31.5	30.3	2182	1402	1.85	0.51	136
M46R18	23.5	22.0	2912	1869	1.96	0.64	163
M46R19	24.3	19.8	2382	1530	1.90	0.64	161
M46R20	25.8	23.8	2661	1705	2.04	0.61	174
M46R21	28.4	25.2	2407	1542	2.08	0.58	188
M46R22	29.3	26.8	2544	1627	2.10	0.58	160
M48R18	23.7	23.1	3311	2127	1.88	0.66	174
M48R19	24.3	21.5	2847	1821	1.77	0.64	160
M48R20	26.2	22.5	2641	1689	2.13	0.61	172
M48R21	28.0	25.6	2687	1722	2.02	0.59	174
M48R22	28.1	27.6	3079	1970	2.14	0.61	171
M50R18	24.2	21.3	2992	1925	1.78	0.68	194
M50R19	24.5	19.5	2638	1695	1.87	0.65	193
M50R20	26.6	25.8	3108	1995	1.97	0.64	170
M50R21	26.9	24.1	2796	1788	2.14	0.61	178
M50R22	29.3	29.0	2997	1918	2.10	0.60	163
M52R18	24.3	21.5	3181	2038	2.06	0.68	181
M52R19	25.7	24.0	3245	2079	2.00	0.66	186
M52R20	26.6	24.0	2975	1910	1.90	0.65	166
M52R21	28.8	27.0	3027	1939	2.05	0.62	172
M52R22	28.0	29.0	3357	2155	1.98	0.61	171
M54R18	24.0	21.8	3369	2158	2.07	0.70	224
M54R19	25.5	24.8	3556	2279	2.00	0.66	195
M54R20	26.3	25.1	3348	2144	2.08	0.65	161
M54R21	27.9	25.1	3017	1935	1.96	0.63	190
M54R22	30.0	26.0	2865	1834	2.15	0.62	198
M60R25	32.1	33.0	3699	2367	2.22	0.62	170
Observations		26.4±0.5	2954±175	2200±90	1.27±0.44	0.38±0.12 (0.64±0.15*)	198±19

Zonoozi et al (2011, MNRAS)

Scenario1: Kroupa IMF – **Pal 14**

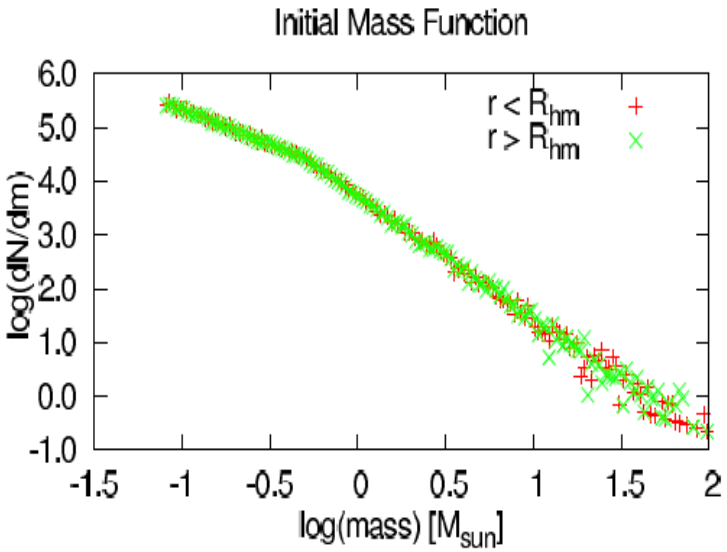

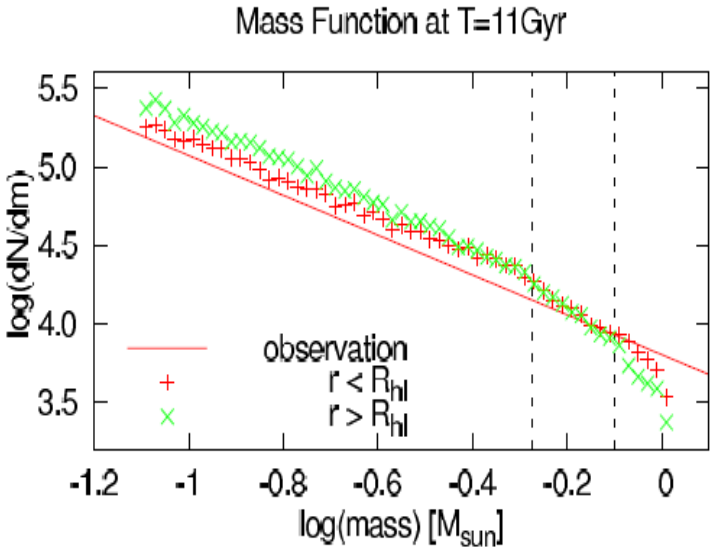

$M^{f}_{r<R_{hm}}[M_\odot]$ (±320)	α (±0.15)	σ_{los}[km/sec] (±0.01)	N_g (±16)
1521	2.10	0.65	162
1402	1.85	0.51	136
1869	1.96	0.64	163
1530	1.90	0.64	161
1705	2.04	0.61	174
1542	2.08	0.58	188
1627	2.10	0.58	160
2127	1.88	0.66	174
1821	1.77	0.64	160
1689	2.13	0.61	172
1722	2.02	0.59	174
1970	2.14	0.61	171
1925	1.78	0.68	194
1695	1.87	0.65	193
1995	1.97	0.64	170
1788	2.14	0.61	178
1918	2.10	0.60	163
2038	2.06	0.68	181
2079	2.00	0.66	186
1910	1.90	0.65	166
1939	2.05	0.62	172
2155	1.98	0.61	171
2158	2.07	0.70	224
2279	2.00	0.66	195
2144	2.08	0.65	161
1935	1.96	0.63	190
1834	2.15	0.62	198
2367	2.22	0.62	170
2200±90	1.27±0.44	0.38±0.12 (0.64±0.15*)	198±19

Zonoozi et al (2011, MNRAS)

Scenario1: Kroupa IMF

Pal 4

Zonoozi et al, 2014

Model	Segregation(S)	R_{phm}[pc]	R_{phl}[pc]	$M^{f}_{r<R_t}$[M$_\odot$]	α_{tot}	α_{in}	α_{out}	σ_{los}[km/sec]
(1)	(2)	(3)	(4)	(5)	(6)	(7)	(8)	(9)
Canonical-NS								
M50R12	0	17.2	16.1	26755	2.30	1.93	2.59	0.81
M55R12	0	17.4	16.1	29372	2.28	2.11	2.62	0.84
M60R12	0	17.3	15.5	32418	2.25	2.01	2.79	0.86
M50R14	0	20.2	16.6	26762	2.25	1.87	2.58	0.76
M55R14	0	20.1	19.0	28506	2.09	1.93	2.54	0.76
M60R14	0	19.5	16.8	32320	2.31	2.17	2.68	0.84
M57R14.5	0	20.4	17.8	30564	2.34	2.18	2.76	0.80
Observation			18.4±1.1	29800±800	1.4±0.25	0.88	1.81	0.87±0.18

The slope is steeper than the observed value

Scenario1: Kroupa IMF

Pal 4

Zonoozi et al, 2014

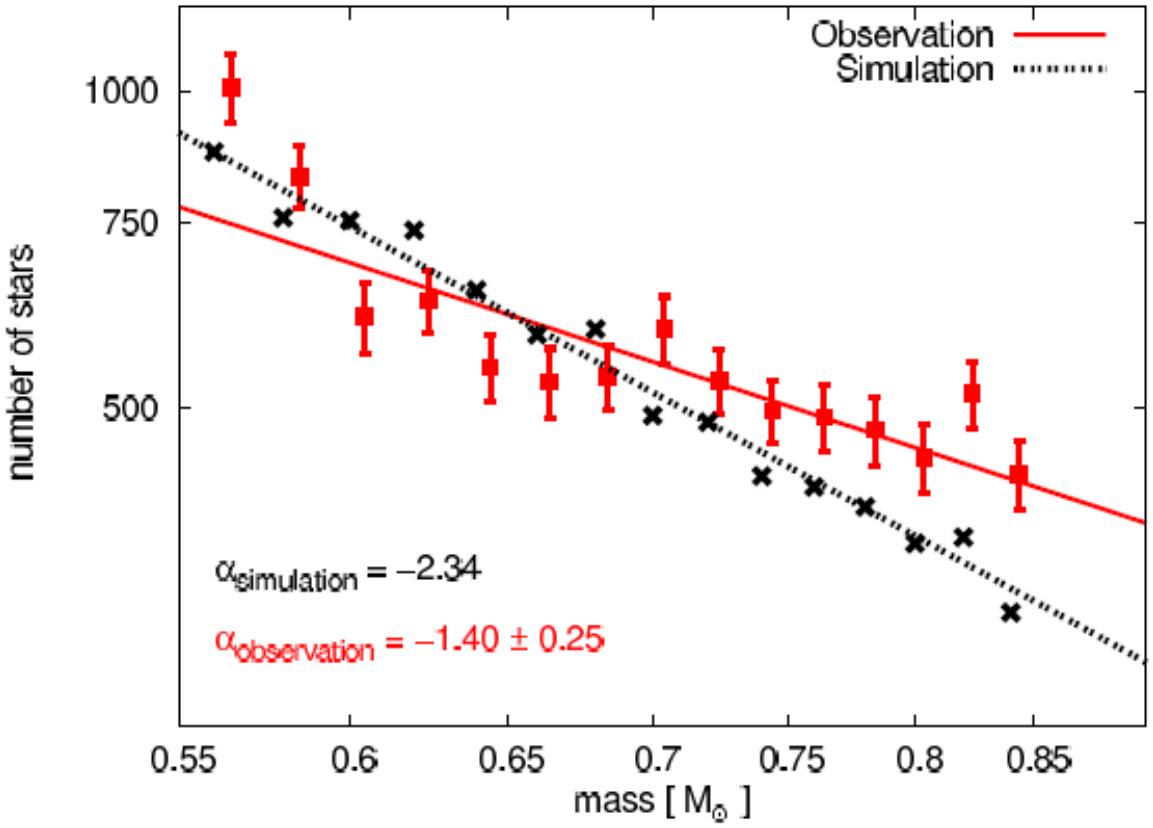

α_{tot}	α_{in}	α_{out}	σ_{los}[km/sec]
(6)	(7)	(8)	(9)
2.30	1.93	2.59	0.81
2.28	2.11	2.62	0.84
2.25	2.01	2.79	0.86
2.25	1.87	2.58	0.76
2.09	1.93	2.54	0.76
2.31	2.17	2.68	0.84
2.34	2.18	2.76	0.80
1.4±0.25	0.88	1.81	0.87±0.18

The slope is steeper than the observed value

Dynamical Mass Segregation

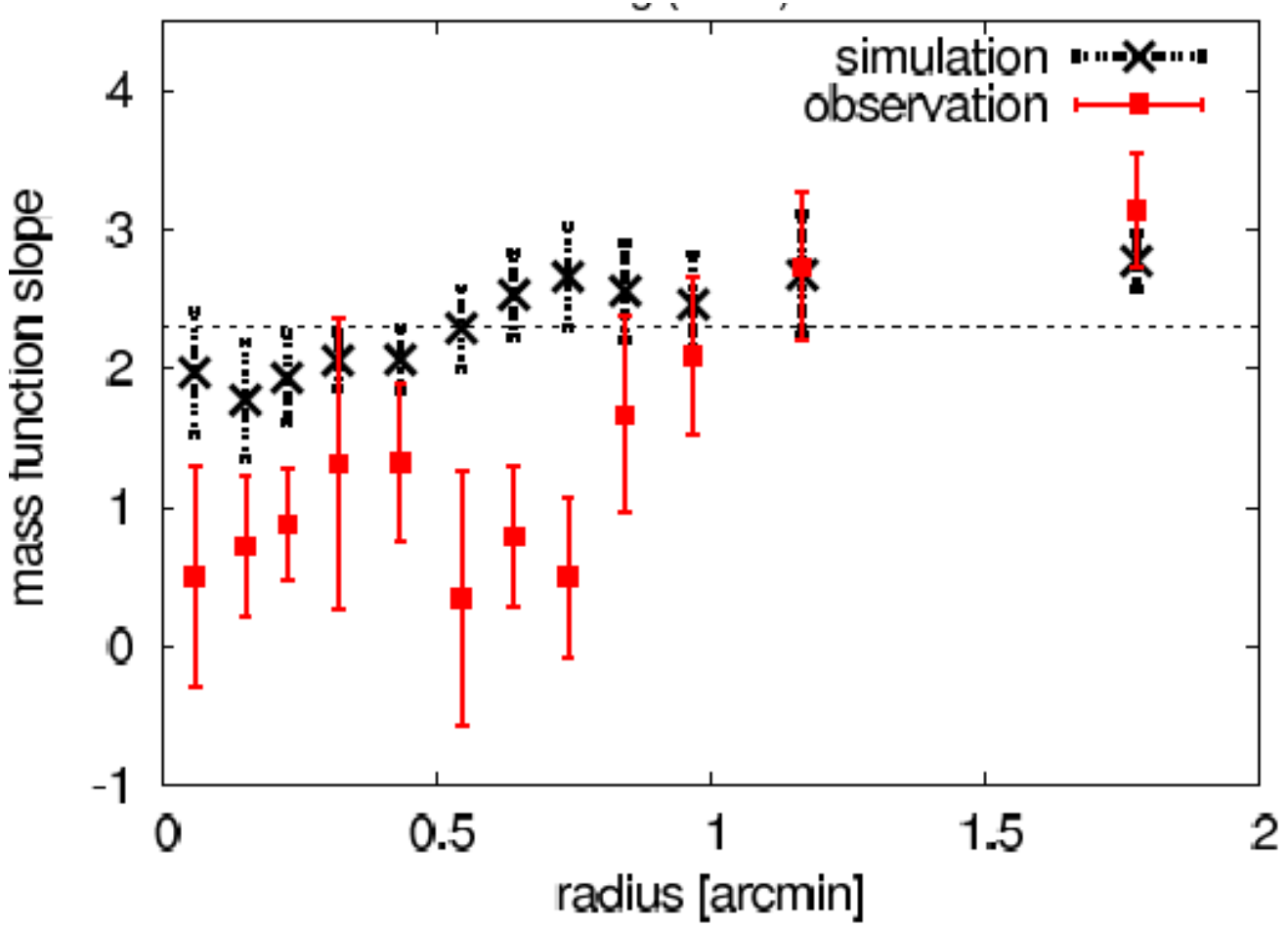

The mass function in the inner part is different from the outer part, but this difference is not as significant as observed value.

Conclusion 1:

Kroupa IMF+ Primordially non-segregated

- **Two-body relaxation** is not able to flatten the mass function sufficiently to reproduce the observations, when starting from canonical Kroupa IMF. Also, it can not explain the segregated structures of these clusters.

- These models do not undergo much **mass loss** due to circular orbit with large galactocentric distance.

Scenario2: Kroupa IMF+ with Primordial segregation

Pal 14

Model	R_{phm} [pc] ±1.2	R_{phl} [pc] ±1.9	N_{bs} ±120	$M^{f}_{r<R_{hm}}$ [$M_\odot$] ±80	α ±0.10	σ_{los}[km/sec] ±0.05	N_g ±8
S0.50M50R20	29.4	25.3	3184	2044	1.90	0.62	193
S0.60M50R20	32.2	27.5	3209	2061	1.9	0.58	207
S0.70M50R20	32.9	27.9	3267	2106	2.0	0.60	191
S0.80M50R20	35.6	29.6	3219	2066	1.95	0.57	222
S0.90M50R20	42.4	36.0	3257	2100	1.6	0.51	211
S0.91M50R20	43.8	38.5	3365	2169	1.63	0.46	206
S0.93M50R20	47.8	40.6	2887	1870	1.27	0.44	217
S0.95M50R20	48.7	41.5	3159	2045	1.28	0.47	215
S0.95M50R15	37.0	27.6	3077	1978	1.33	0.58	194
S0.90M50R15	33.9	26.3	3236	2085	1.67	0.55	210
B0.04M50R20	27.4	25.3	3132	2009	2.0	0.87	185
Observations		26.4±0.5	2954±175	2200±90	1.27±0.44	0.38±0.12 (0.64±0.15*)	198±19

Clusters with such a strong degree of primordial mass segregation are able to reproduce the observed flat mass function **inside the half-light radius**.

Zonoozi et al 2011, MNRAS

Scenario2: Kroupa IMF+ with Primordial segregation

Pal 14

Model	N_g ±8
S0.50M50R	193
S0.60M50R	207
S0.70M50R	191
S0.80M50R	222
S0.90M50R	211
S0.91M50R	206
S0.93M50R	217
S0.95M50R	215
S0.95M50R	194
S0.90M50R	210
B0.04M50R	185
Observatio	198±19

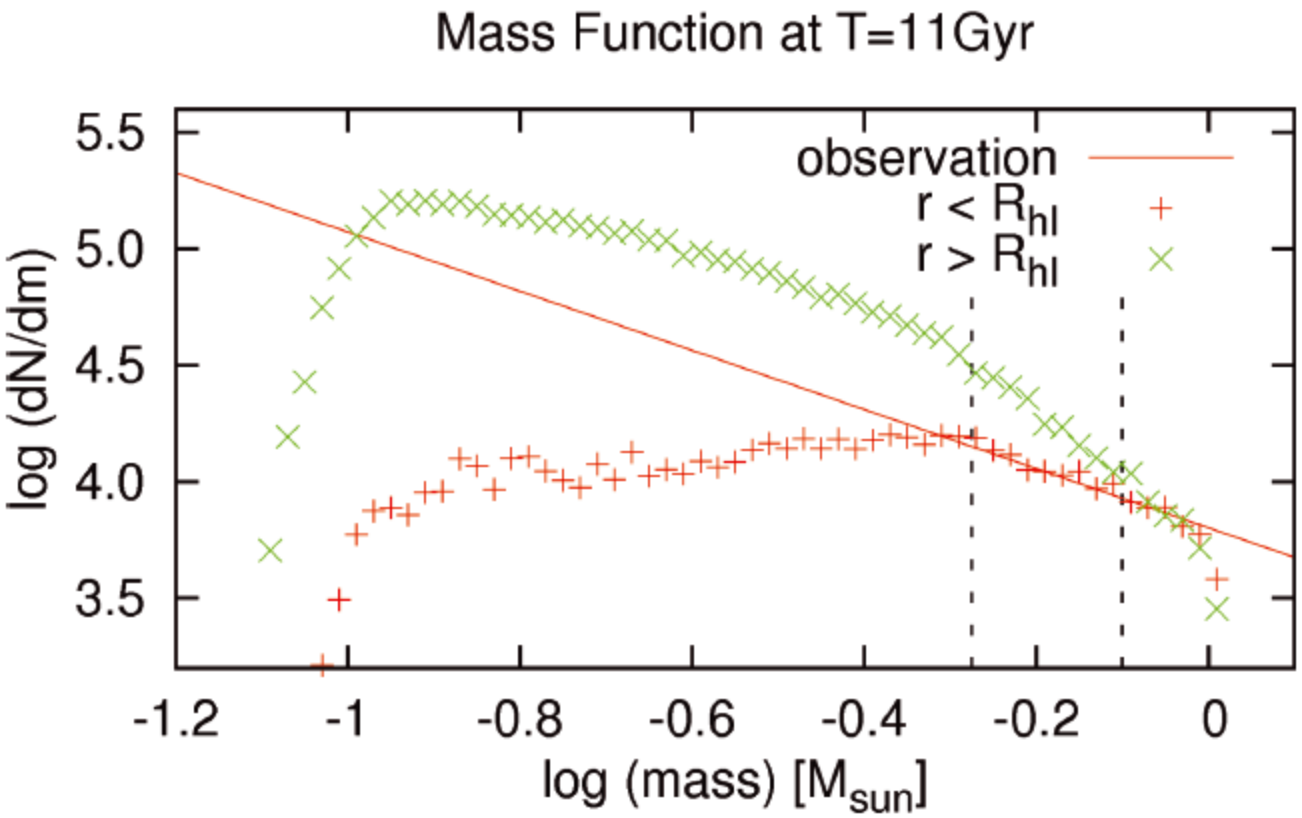

Clusters with such a strong degree of primordial mass segregation are able to reproduce the observed flat mass function **inside the half-light radius**.

Zonoozi et al 2011, MNRAS

Scenario2: Kroupa IMF+ with Primordial segregation

Pal 4

Clusters with various degree of primordial mass segregation are still not able to reproduce the observed flat mass function

Model	R_{phm}[pc]	R_{phl}[pc]	$M^{f}_{r<R_t}$[$M_\odot$]	α_{tot}	α_{in}	α_{out}	σ_{los}[km/sec]
(1)	(2)	(3)	(4)	(5)	(6)	(7)	(8)
Canonical-S							
S0.50M60R10	16.8	13.3	32125	2.27	1.84	2.81	0.88
S0.80M60R8	17.1	12.3	32739	2.27	1.94	3.00	0.87
S0.95M60R8	21.0	16.5	32606	2.10	1.68	2.89	0.79
S0.95M60R10	28.2	20.8	31422	2.19	1.61	3.19	0.69
S0.95M55R9	26.5	20.8	27901	2.22	1.76	2.86	0.67
S0.95M57R10	27.8	19.1	29947	2.20	1.81	2.94	0.69
Observation		18.4±1.1	29800±800	1.4±0.25	0.88	1.81	0.87±0.18 (1.15±0.20*)

Scenario2: Kroupa IMF+ with Primordial segregation

Pal 4

Almost the whole cluster is included for calculation of the global mass function

Model	R_{phm} [pc]
(1)	(2)
Canonical-S	
S0.50M60R10	16.8
S0.80M60R8	17.1
S0.95M60R8	21.0
S0.95M60R10	28.2
S0.95M55R9	26.5
S0.95M57R10	27.8
Observation	

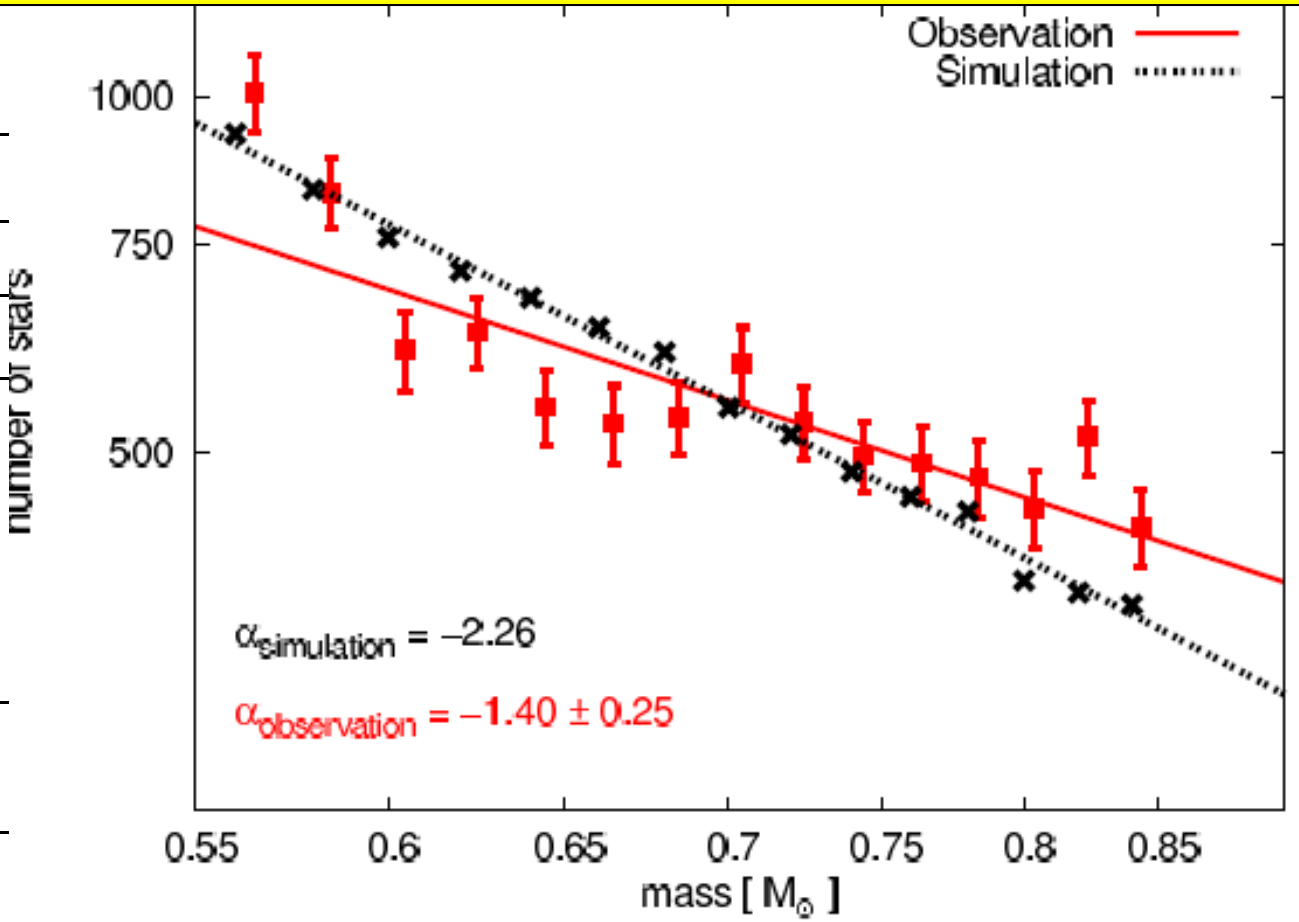

Scenario3: Flattened IMF+with Primordial segregation

Pal 4

Model	Segregation(S)	R_{phm}[pc]	R_{phl}[pc]	$M^{f}_{r<R_t}$[$M_\odot$]	α_{tot}	α_{in}	α_{out}	σ_{los}[km/sec]
Flattened-S								
F0.6S0.90M57R10	0.90	22.9	20.3	30231	1.41	0.79	2.35	0.76
F0.6S0.70M55R10	0.70	18.6	16.8	29418	1.53	1.23	2.22	0.80
F0.6S0.70M57R12	0.70	22.0	20.5	30457	1.61	1.38	2.28	0.77
F0.6S0.50M57R10	0.50	16.8	15.5	30484	1.51	1.40	2.06	0.86
Observation			18.4±1.1	29800±800	1.4±0.25	0.88	1.81	0.87±0.18

Scenario3: Flattened IMF+with Primordial segregation

Pal 4

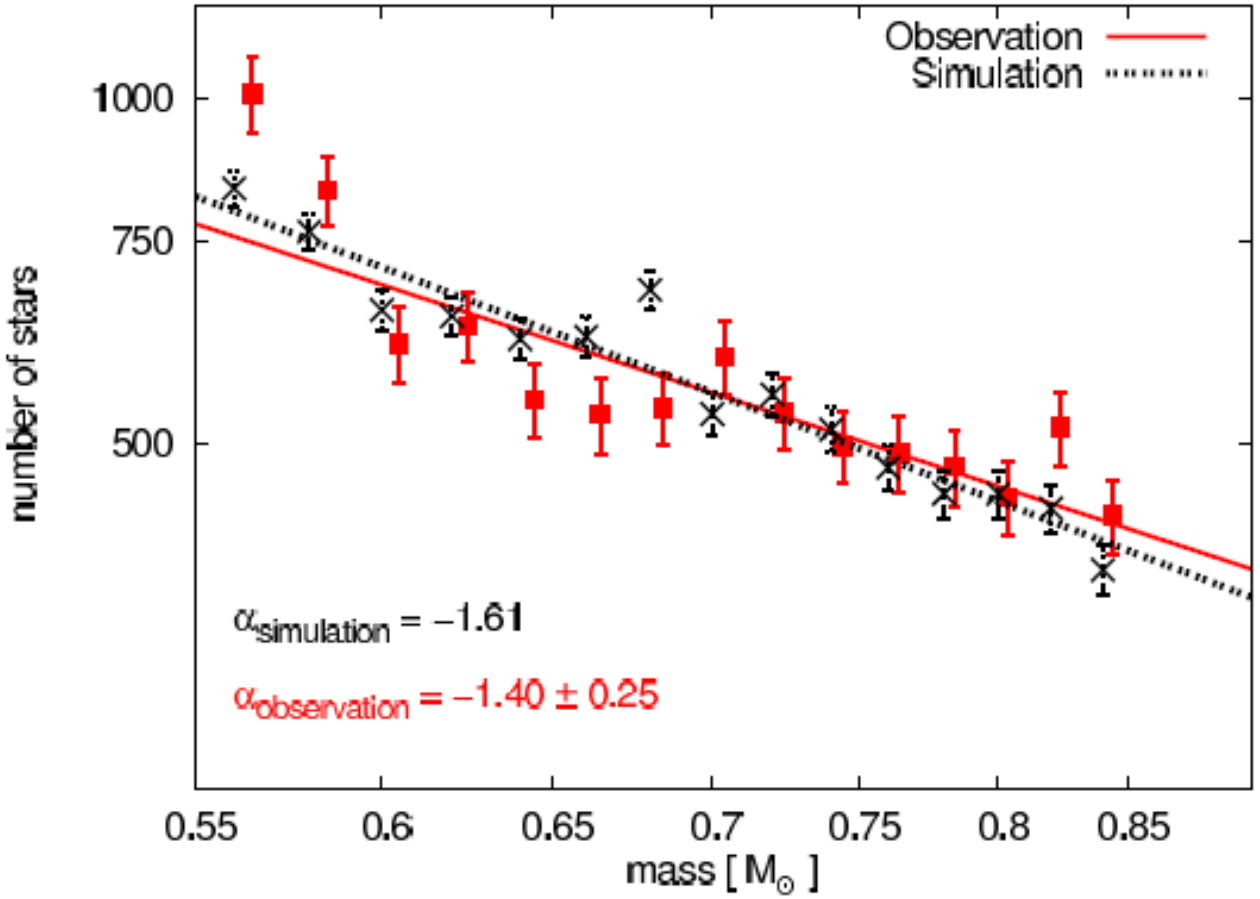

ɔt	α_{in}	α_{out}	σ_{los}[km/sec]
.41	0.79	2.35	0.76
.53	1.23	2.22	0.80
.61	1.38	2.28	0.77
.51	1.40	2.06	0.86
±0.25	0.88	1.81	0.87±0.18

- Fits the observed global MF very well .
- Observed mass segregation profile is matched very well by simulation

Scenario3: Flattened IMF+with Primordial segregation

Pal 4

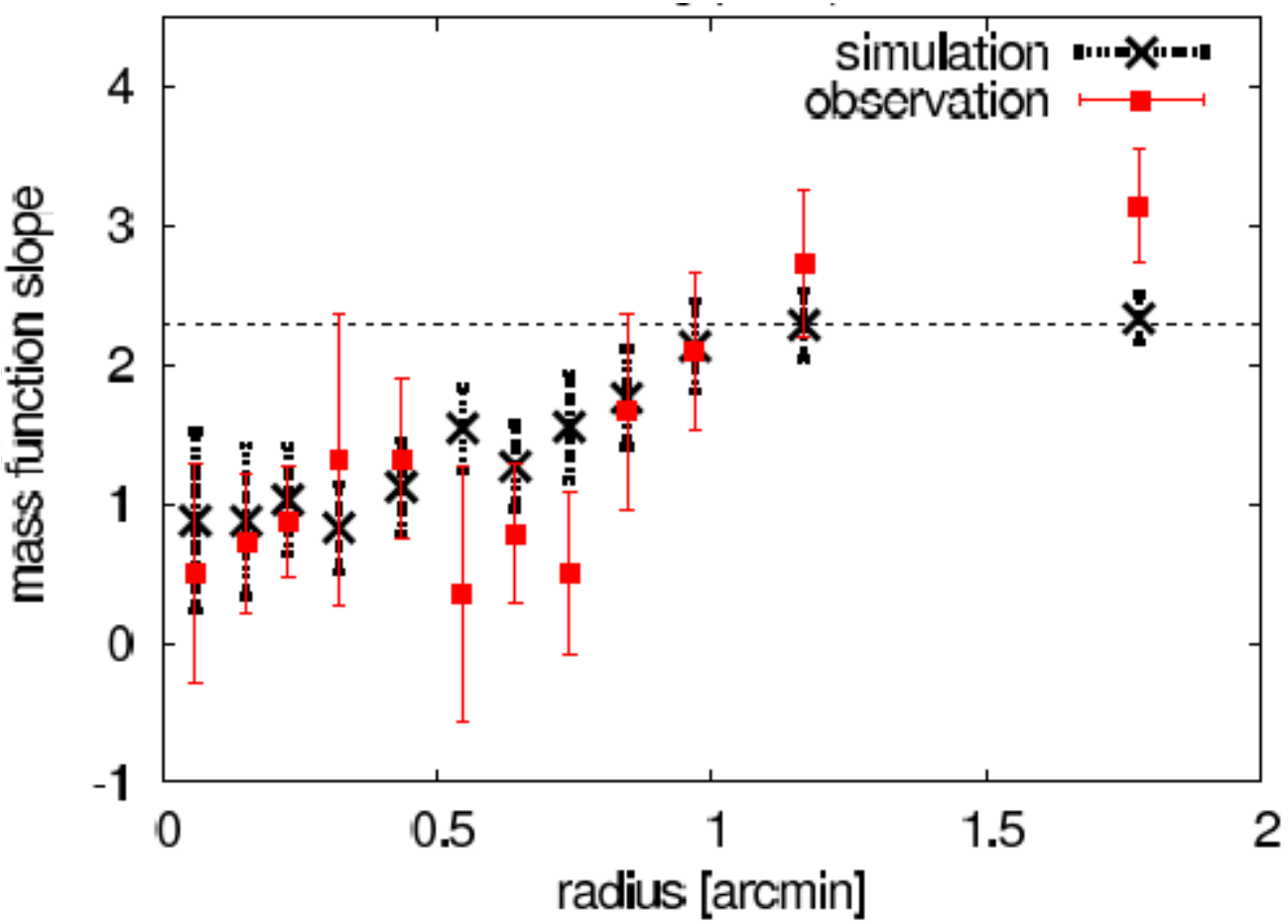

	α_{in}	α_{out}	σ_{los}[km/sec]
	0.79	2.35	0.76
	1.23	2.22	0.80
	1.38	2.28	0.77
	1.40	2.06	0.86
25	0.88	1.81	0.87±0.18

- Fits the observed global MF very well .
- Observed mass segregation profile is matched very well by simulation

The effect of unresolved binaries

- Binary stars, either primordial or dynamically formed during close encounters between single stars, can affect the observational parameters of a star cluster, such as velocity dispersion and mass function.

- If any of the stars in a sample are members of a binary system, their measured magnitude will be decreased and consequently yielded to the larger mass.

(Kroupa & Tout 1992, MNRAS)

The effect of unresolved binaries

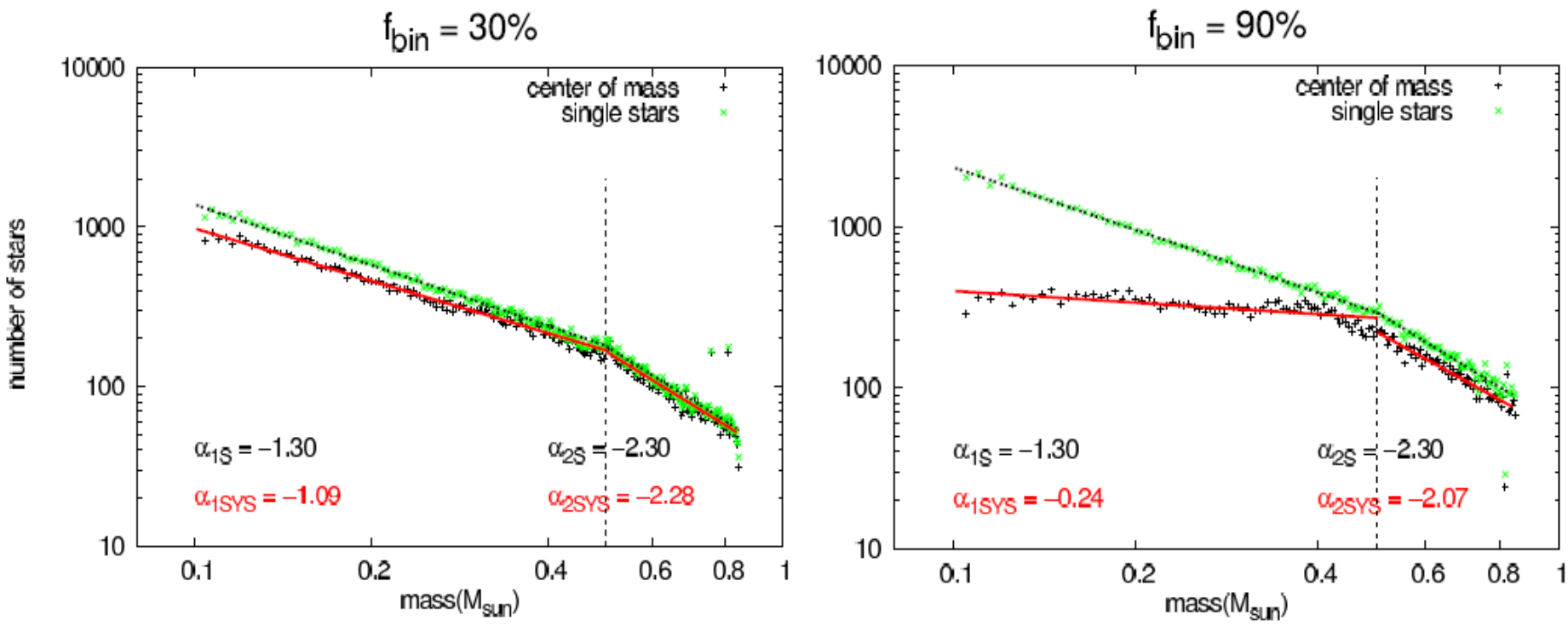

The effect of binarity on the measured mass function

The slope of the mass function in the **low mass** range decreases as the binary fraction increases (low masses are hidden by heave star), while there is no significant change in the **high-mass end which is the observed range** in this paper.

Scenario 4

Eccentric Orbit

(Zonoozi et al. in preparation)

Kroupa IMF+ without any extreme ICs

Eccentric orbits causes higher mass loss

Kuepper et al 2014, Webb et al 2014

Evolution of mass function

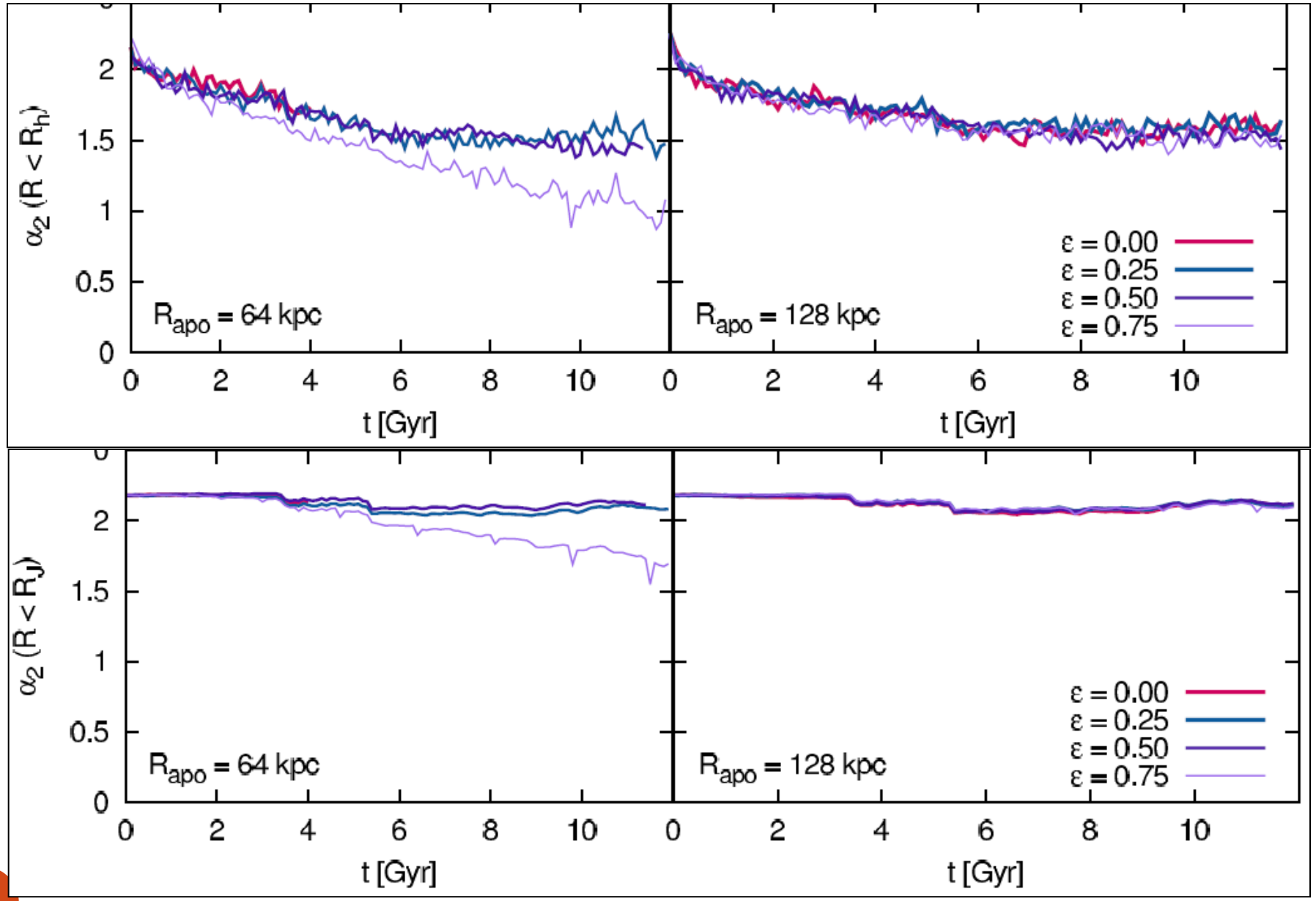

Kuepper et al , In preparation

Eccentric orbit for Palomar 4

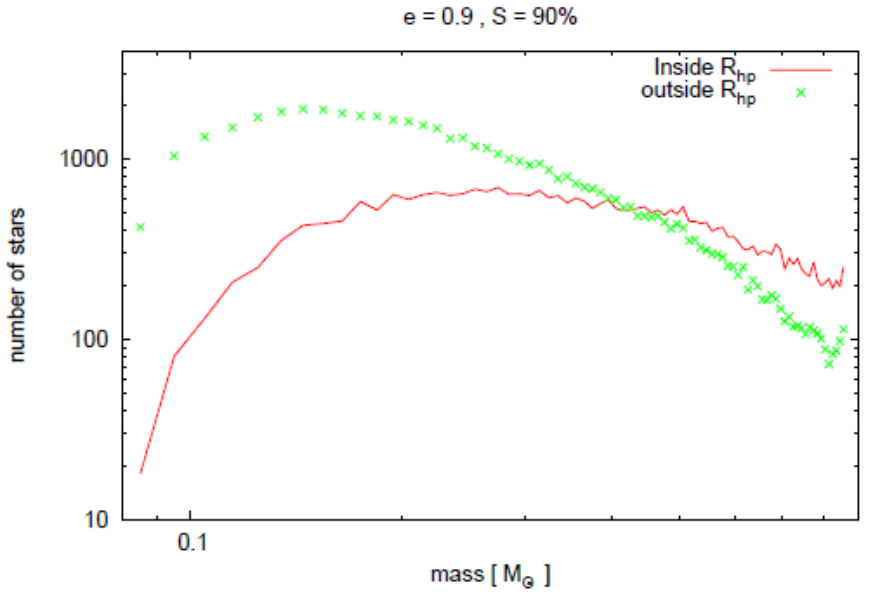

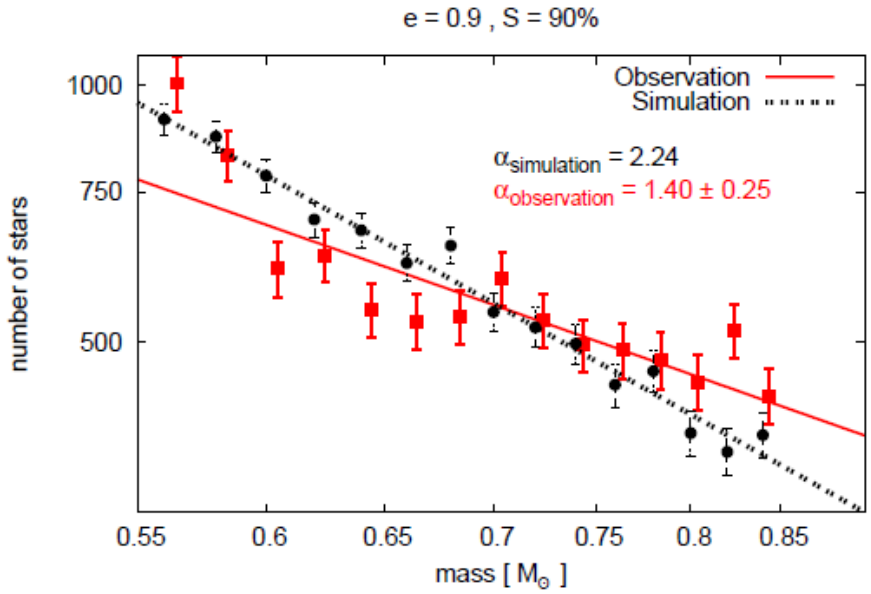

R_{apo}=100 kpc

R_{per}=10 kpc

Ni=180,000 stars

Nf=80,000 stars

Mi= 90,000

Mf=30,000

$R_{h,i}$ = 8 pc

$R_{h,i}$ = 17 pc

Conclusion

- We found the most likely starting conditions of Pal 4 and Pal14.

- We showed that models evolving on circular orbits, starting with a Kroupa IMF, and without primordial mass segregation do not produce enough flattening / mass segregation in the slope of the mass function.

- The observed mass function may be the result of an already established non-canonical IMF depleted in low-mass stars, which might have been obtained during a violent early phase of gas expulsion of an embedded cluster with primordial mass segregation.

- We found that the effect of unresolved binaries can not be responsible for the flattening of the mass function in the observed mass range.

- We showed that even extreme eccentric orbit can not reproduce such amount of flattening in Pal 4 and Pal 14.

Of course , we are still looking for eccentric orbits…….